

# Enhancing Autonomous Online Intrusion Detection for IoT with Balanced Learning, Reliable Pseudo-Labels, and Lightweight Architectures

Hanzala Afzaal<sup>a</sup>, Danish Memon<sup>a</sup>, Chouhdary Bilal Raza<sup>a</sup>, Dr Muhammad Khurram Shahzad<sup>a</sup>

<sup>a</sup>*School of Electrical Engineering and Computer Science (SEECs),  
National University of Sciences and Technology (NUST), Islamabad, Pakistan*

## Abstract

The rapid proliferation of Internet of Things (IoT) devices has created an urgent demand for adaptive, resource-efficient Intrusion Detection Systems (IDS) capable of handling dynamic and evolving cyber threats. This paper investigates AOC-IDS, a state-of-the-art autonomous online IDS published at IEEE INFOCOM 2024, which employs an Autoencoder (AE) with Cluster Repelling Contrastive (CRC) loss and an autonomous Gaussian-based decision module. We first successfully replicate AOC-IDS on the UNSW-NB15 benchmark, achieving 89.39% accuracy in close agreement with the published 89.19%. We then systematically identify four key limitations class imbalance, unreliable pseudo-label generation, limited generalization, and computational overhead for IoT deployment and propose targeted improvements for each. Our *XGBoost-BalSamp*, applying XGBoost with domain-specific feature engineering and a balanced sampling strategy, achieves 95.45% accuracy on UNSW-NB15, a gain of +6.26% over the baseline. Our combined deep learning improvement (*PseudoFilter* + *MixupAug* + *LiteAE*), incorporating confidence-filtered pseudo-labels with encoder-decoder agreement voting, Mixup data augmentation, and a lightweight model architecture, achieves a best-run accuracy of 90.88% (F1: 91.45%), surpassing the base paper by +1.69% (F1: +1.31%). Individual ablation shows each component contributes positively: *PseudoFilter* alone yields ~90.44%, *MixupAug* adds ~0.61% through Mixup augmentation, and *LiteAE* reduces parameter count by 55% while maintaining competitive accuracy. Our results demonstrate that targeted, principled improvements to AOC-IDS yield consistent accuracy gains while also improving practical deployability on IoT edge devices. **Code Repository:** <https://github.com/danishmemon847/AOC-IDS-Pipeline>

**Keywords:** Intrusion Detection System, IoT Security, Online Learning, Contrastive Learning, Class Imbalance, XGBoost, Pseudo-labels, UNSW-NB15, Mixup Augmentation, Lightweight Architecture

## 1. Introduction

The exponential growth of the Internet of Things (IoT) has transformed industries ranging from smart manufacturing to health-care and transportation [1, 2, 3]. By 2024, billions of IoT devices were estimated to be active globally, many operating in safety-critical environments where a successful intrusion can have severe physical or financial consequences. However, this growth has simultaneously created an expanding attack surface. IoT malware attacks have increased sharply year on year, with millions of devices targeted globally [4]. Unlike traditional computing environments, IoT systems operate under tight resource constraints limited memory, processing power, and battery life often without the capacity for heavy-weight security solutions [5]. Intrusion Detection Systems (IDS) form a critical layer of defense for IoT networks. They can be broadly classified into two categories: signature-based detection, which identifies known threats by matching against a predefined library, and anomaly-based detection, which learns the normal behavioral profile of the system and raises alerts upon deviation from that profile. Anomaly-based IDS are particularly valuable in this context, as they detect deviations from learned normal behavior without requiring a database of known attack signatures, making them capable of identifying zero-day threats [6].

The application of deep learning has significantly advanced the capability of anomaly-based IDS, enabling richer and more discriminative representations of network traffic patterns [7]. AOC-IDS, proposed by Zhang et al. [8] at IEEE INFOCOM 2024, represents a significant advance in online, autonomous IDS for IoT environments. It introduces a novel Autoencoder (AE) architecture trained with a Cluster Repelling Contrastive (CRC) loss, a Gaussian-based autonomous decision-making module, and an online learning framework that generates pseudo-labels without human intervention. By eliminating the need for manual labeling, AOC-IDS greatly reduces deployment overhead in dynamic environments. The system achieves 89.19% accuracy on UNSW-NB15 and 88.90% on NSL-KDD, outperforming prior state-of-the-art methods. Despite its strong performance, AOC-IDS exhibits four concrete limitations that constrain its real-world applicability: it does not handle class imbalance in the training data, its pseudo-label generation lacks a quality filtering mechanism, it applies no data augmentation for generalization, and its model size exceeds the memory constraints of many IoT edge devices.

This paper makes the following contributions:

1. We successfully replicate AOC-IDS on UNSW-NB15 using the official repository and published hyperparame-

ters, achieving 89.39% accuracy, confirming reproducibility of the base system.

2. We identify and formally characterize four concrete limitations of AOC-IDS: class imbalance handling, pseudo-label reliability, generalization to unseen traffic, and IoT resource overhead.
3. We propose and evaluate *XGBoost-BalSamp* XGBoost with domain-specific feature engineering and balanced sampling achieving 95.45% accuracy, a gain of +6.26% over the base paper.
4. We propose and evaluate *PseudoFilter*, *MixupAug*, and *LiteAE* individually and in combination, achieving a best-run accuracy of 90.88% (F1: 91.45%) with a 55% reduction in model parameters from 67,202 to 29,830.
5. We conduct a comprehensive ablation study with all pairwise and combined configurations, and compare against all baseline methods used in the original AOC-IDS paper, demonstrating consistent superiority.

The remainder of this paper is organized as follows. Section 2 reviews related work. Section 3 provides an overview of the base AOC-IDS system. Section 4 identifies limitations. Section 5 describes the proposed methodology. Section 6 details the proposed improvements. Section 7 presents the experimental setup. Section 8 reports results and discussion. Section 9 concludes the paper.

## 2. Related Work

### 2.1. Machine Learning for Intrusion Detection

Machine learning methods have been widely applied to network intrusion detection [9]. Classical approaches including Support Vector Machines (SVM) and Random Forests demonstrated promising results on benchmark datasets [10, 11], providing strong baselines for the field. A shared weakness of such static approaches is that any shift in the threat landscape demands full model retraining, rendering them poorly suited to the continuously changing attack surface of IoT deployments. Architectures such as Convolutional Neural Networks (CNNs) and Recurrent Neural Networks (RNNs) pushed detection performance further by learning hierarchical representations of network traffic directly from raw data [12, 13]. Nevertheless, these models are fundamentally offline: they cannot incorporate newly observed attack patterns without discarding and rebuilding the learned model from scratch.

### 2.2. Contrastive Learning in Security

Contrastive learning has emerged as a powerful paradigm for learning discriminative representations in security applications. FeCo [14] applies InfoNCE-style contrastive loss to intrusion detection, maximizing the distance between benign and malicious representations while clustering benign samples. CIDS [15] combines contrastive and cross-entropy loss to improve intra-class cohesion and inter-class separation. Lopez-Martin et al. [16] apply contrastive learning with random Fourier features specifically for IoT IDS, demonstrating that contrastive approaches

outperform purely supervised methods when labeled data is scarce. These works collectively motivate the use of contrastive loss in the AOC-IDS framework we build upon.

### 2.3. Online Learning for IoT IDS

Online learning enables IDS to adapt to dynamic environments where normal and malicious behavior evolve over time [17]. Unlike offline models that assume a static data distribution, online learning frameworks update model parameters incrementally as new data arrives. Han et al. [18] reduce labeling overhead by selectively labeling only the most influential samples, showing that not all incoming data carries equal training value. Yang and Shami [5] tackled this challenge by designing a lightweight drift-detection mechanism tuned specifically for IoT data streams, underscoring that recognising distribution shifts early is as important as updating the model in response. Complementing this, Gyamfi and Jurcut [19] built an industrial IoT IDS that triggers incremental re-training whenever novel attack behaviour is detected. Taken together, these studies make a compelling case for IDS solutions that are both adaptive and computationally frugal.

### 2.4. Class Imbalance and Data Augmentation

Class imbalance is a persistent obstacle in network intrusion detection [20]: attack traffic is often vastly outnumbered by benign flows, and models trained on such skewed distributions tend to favour the majority class at the expense of attack recall. XGBoost [21] is naturally resistant to this bias because its gradient-boosting objective assigns higher weight to misclassified minority samples at each boosting round. Oversampling via SMOTE [20] complements this by synthetically expanding the minority class so the training distribution becomes more balanced. Mixup augmentation [22] takes a different angle: by interpolating pairs of training examples, it pushes the model towards smoother decision boundaries and thereby reduces over-reliance on the particular statistics of the training corpus. All three approaches inform the improvements developed here.

## 3. AOC-IDS: Base System Overview

### 3.1. System Architecture

AOC-IDS [8] comprises two tightly integrated components: the Anomaly Detection Module (ADM) and the Online Learning Framework. The ADM uses a symmetric Autoencoder with layer dimensions [196  $\rightarrow$  128  $\rightarrow$  64  $\rightarrow$  128  $\rightarrow$  196], where the bottleneck layer at dimension 64 compresses input network traffic features into a compact latent representation. The encoder and decoder outputs are both used for classification, a design choice that increases representational diversity within a single forward pass.

### 3.2. Cluster Repelling Contrastive (CRC) Loss

The CRC loss is the core training objective of the ADM. It is derived from the standard InfoNCE loss [24] but modified to produce a dual-category repulsion effect tailored to binary

intrusion detection. For a normal anchor representation  $v_{n,i}$ , the per-pair loss is:

$$\mathcal{L}_{ij} = -\log \frac{\exp(\text{sim}(i, j)/\tau)}{\exp(\text{sim}(i, j)/\tau) + \sum_i \sum_k \exp(\text{sim}(i, k)/\tau)} \quad (1)$$

where  $\text{sim}(i, j) = \text{CosSim}(v_i, v_j)$  is the cosine similarity between representation vectors and  $\tau=0.02$  is the temperature hyperparameter. The full loss averages  $\mathcal{L}_{ij}$  over all normal pairs  $(i, j)$  in the training batch. Unlike standard InfoNCE, which repels negative samples from a single anchor, CRC traverses all anchors in the normal class simultaneously, ensuring that attack representations are repelled from all normal cluster centers at each training step. The final loss combines encoder and decoder losses:  $\mathcal{L}_{\text{final}} = \mathcal{L}^{\text{en}} + \mathcal{L}^{\text{de}}$ .

### 3.3. Gaussian Decision-Making Module

After training, the ADM computes cosine similarity scores between the average normal representation and all training data representations. These scores are modeled as a mixture of two Gaussian distributions using Maximum Likelihood Estimation (MLE): one Gaussian for normal traffic (higher mean) and one for attack traffic (lower mean). At inference, each test sample is classified by the Gaussian with higher posterior probability. This autonomous, threshold-free decision process is a key advantage over methods like FeCo [14] that require manual threshold calibration. Both the encoder and decoder independently produce a classification, and a voting mechanism selects the prediction with higher confidence as the final output.

### 3.4. Online Learning Framework

The online framework enables continuous adaptation without human labeling. It operates in two repeating phases. In the pseudo-label generation phase, new unlabeled samples arriving in a stream are passed through the current ADM to generate pseudo-labels. In the system adaptation phase, the ADM is fine-tuned on the expanded dataset comprising both original labeled data and the newly pseudo-labeled samples for  $\text{epoch}_1 = 3$  epochs per batch. The framework processes data in batches of 2,784 samples (1.6% of UNSW-NB15), initially training on 20% of labeled data. A random flip of  $\lambda=5\%$  of pseudo-labels per batch introduces controlled noise to prevent the model from overfitting to its own wrong judgments, and the Gaussian distributions are always computed using only the clean initial labeled dataset to maintain a reliable reference point.

### 3.5. Base Paper Replication

To establish a reliable baseline for our improvements, we cloned the official AOC-IDS GitHub repository and executed it with the exact published hyperparameters: SGD optimizer, learning rate = 0.001, batch size = 128,  $\text{epoch}_0=300$ ,  $\text{epoch}_1=3$ ,  $\lambda=5\%$ . Our replication yielded 89.39% accuracy and 90.12% F1 on UNSW-NB15, against the published figures of 89.19% accuracy and 90.14% F1. The +0.20% accuracy gap is consistent with ordinary stochastic variation across runs and therefore

validates the reproducibility of the original system. All subsequent comparisons in this paper are made against these replicated numbers rather than the published values, ensuring a fully controlled experimental reference point.

## 4. Identified Limitations

A careful reading of the AOC-IDS design, combined with observations gathered during replication, revealed four specific weaknesses that limit both detection quality and practical deployment in real IoT settings.

### 4.1. Limitation 1: Class Imbalance

The UNSW-NB15 training partition holds roughly 56,000 normal records against 119,341 attack records, giving an attack-to-normal ratio of approximately 2.1:1. AOC-IDS applies no balancing strategy at any training stage. Because attack samples dominate the cosine-similarity score distribution, the fitted Gaussians can fail to draw a clean boundary between normal and malicious traffic, pushing the operating point toward higher false-positive or false-negative rates depending on which class skews the distribution. The CRC loss partially compensates by attending to representation geometry rather than raw counts, but this does not substitute for an explicit correction of the sampling imbalance.

### 4.2. Limitation 2: Pseudo-label Noise Accumulation

The only mechanism for handling incorrect pseudo-labels in AOC-IDS is a 5% random label flip, which diversifies errors but does not selectively reject low-confidence predictions. In our experiments, accuracy fell from around 90% at the fifth streaming batch to approximately 75% at the fiftieth. The root cause is straightforward: every incorrectly labelled sample is permanently admitted to the training set without any quality gate, so the model is trained on progressively noisier supervision. Over many batches the accumulated label noise outpaces the corrective effect of the random flip, producing a gradual but severe accuracy collapse in the later phase of online training.

### 4.3. Limitation 3: Poor Generalization to Unseen Traffic

AOC-IDS trains solely on the samples present in the initial labelled pool and the incoming pseudo-labelled stream, with no augmentation of any kind. Live IoT traffic deviates from benchmark recordings in subtle but consequential ways: protocols evolve, device firmware changes, and temporal usage patterns shift. Exposure only to the benchmark’s fixed statistical footprint leaves the model susceptible to overfitting those particular characteristics, which undermines generalisation when the system is eventually deployed on production networks whose traffic distribution differs from UNSW-NB15.

#### 4.4. Limitation 4: Computational Overhead for IoT Edge Deployment

Storing a 67,202-parameter model in 32-bit floating point requires roughly 263 KB of RAM. For cloud servers this is negligible, but many widely deployed edge microcontrollers including the Arduino Mega (8 KB SRAM) and the ESP8266 (80 KB RAM) cannot accommodate a model of this size. Even on more capable edge boards, a leaner architecture translates directly into shorter inference latency and reduced energy draw, both of which matter greatly when the device runs on a battery. The base AE therefore stands as a practical barrier to on-device execution without some form of architectural compression.

## 5. Methodology

Figure 1 illustrates the complete research pipeline.

### 5.1. Research Pipeline Overview

Our methodology follows a five-stage pipeline as illustrated in Figure 1: (1) Base system replication to confirm reproducibility; (2) Limitation analysis to identify and characterize weaknesses; (3) Improvement design, where each limitation is addressed by a targeted technique; (4) Individual evaluation, testing each improvement in isolation; and (5) Combined evaluation, testing all three deep learning improvements together to assess their complementary effects.

### 5.2. XGBoost-BalSamp: Addressing Class Imbalance

XGBoost is selected as the backbone for Improvement 1 due to its native handling of tabular features and its gradient boosting objective, which adaptively up-weights misclassified samples and implicitly handles moderate class imbalance. To further strengthen its ability to discriminate between normal and attack traffic, we construct three domain-specific composite features from the raw UNSW-NB15 attributes: `total_load = sload+dload` (combined source and destination load), `rate_ratio = sbytes/(dur + 0.001)` (source byte rate, with small epsilon to prevent division by zero), and `pkt_diff = spkts - dpkts` (packet asymmetry, a known indicator of scanning and DoS behavior). A stratified 80/20 resplit of the UNSW-NB15 training set ensures proportional representation of all 9 attack categories in both training and validation subsets.

### 5.3. PseudoFilter: Addressing Pseudo-label Noise

PseudoFilter introduces a dual-gate quality control mechanism that replaces the blind acceptance of all pseudo-labels in the base system. A pseudo-label is accepted for training only when *both* of the following conditions are satisfied: (A) the sigmoid output confidence of the prediction is at least 0.85, meaning the model is highly certain of its decision, and (B) the encoder-side classifier (`clf_enc`) and decoder-side classifier (`clf_dec`) independently produce the same prediction (encoder-decoder agreement voting). If either condition fails, the sample is assigned the conservative default label of 0 (normal) rather than being added to the training set with a potentially incorrect

attack label. This design ensures that only the subset of samples where the model is both confident and internally consistent contributes to online model updates, directly attacking the root cause of the accuracy collapse observed in the base system.

### 5.4. MixupAug: Addressing Poor Generalization

MixupAug integrates Mixup data augmentation [22] into every training batch. Each virtual sample is formed by a convex blend of two randomly selected examples:  $\tilde{x} = \lambda x_i + (1-\lambda)x_j$  and  $\tilde{y} = \lambda y_i + (1-\lambda)y_j$ , with the mixing weight  $\lambda \sim \text{Beta}(0.2, 0.2)$ . Choosing  $\alpha=0.2$  for the Beta distribution produces a U-shaped density heavily concentrated near 0 and 1, so the majority of generated samples sit close to one of their two parents and only a small fraction interpolate deeply between classes. The practical effect is that decision boundaries become smoother and less anchored to individual training examples, making the model more robust when real-world IoT traffic deviates from the benchmark distribution.

### 5.5. LiteAE: Addressing IoT Computational Overhead

LiteAE reduces the Autoencoder’s hidden layer dimensions from [128, 64] to [64, 32], giving a new architecture of [194  $\rightarrow$  64  $\rightarrow$  32  $\rightarrow$  64  $\rightarrow$  194]. This reduces the total parameter count from 67,202 to 29,830, a reduction of 55.6%, and memory footprint from approximately 263 KB to approximately 117 KB in float32. BatchNorm layers and dual classifier heads (`clf_enc`, `clf_dec`) are retained to preserve the architectural advantages of the original system. Since smaller networks are more sensitive to learning rate scheduling, we replace the fixed learning rate of the base system with cosine annealing ( $\eta_{\min}=10^{-5}$ ,  $T_{\max}=50$ ), which gradually reduces the learning rate over cycles to ensure stable convergence of the compact architecture.

### 5.6. Combined System Design

The three deep learning improvements *PseudoFilter*, *MixupAug*, and *LiteAE* are designed to compose without conflict. *LiteAE* defines the model architecture; *MixupAug* modifies the training batch construction; and *PseudoFilter* controls which pseudo-labeled samples are accepted during online updates. These three stages operate at different points in the training pipeline and therefore do not interfere with one another. Their combined interaction is depicted in Figure 2.

## 6. Proposed Improvements: Implementation Details

### 6.1. XGBoost-BalSamp

The XGBoost model is configured with 1,000 estimators, a learning rate of 0.05, maximum tree depth of 10, subsample ratio of 0.8, and `tree_method='hist'` for computational efficiency. Early stopping with a patience of 50 rounds on the validation set prevents overfitting. No explicit class weight parameter (`scale_pos_weight`) is applied, as the gradient boosting mechanism combined with balanced sampling provides sufficient correction.

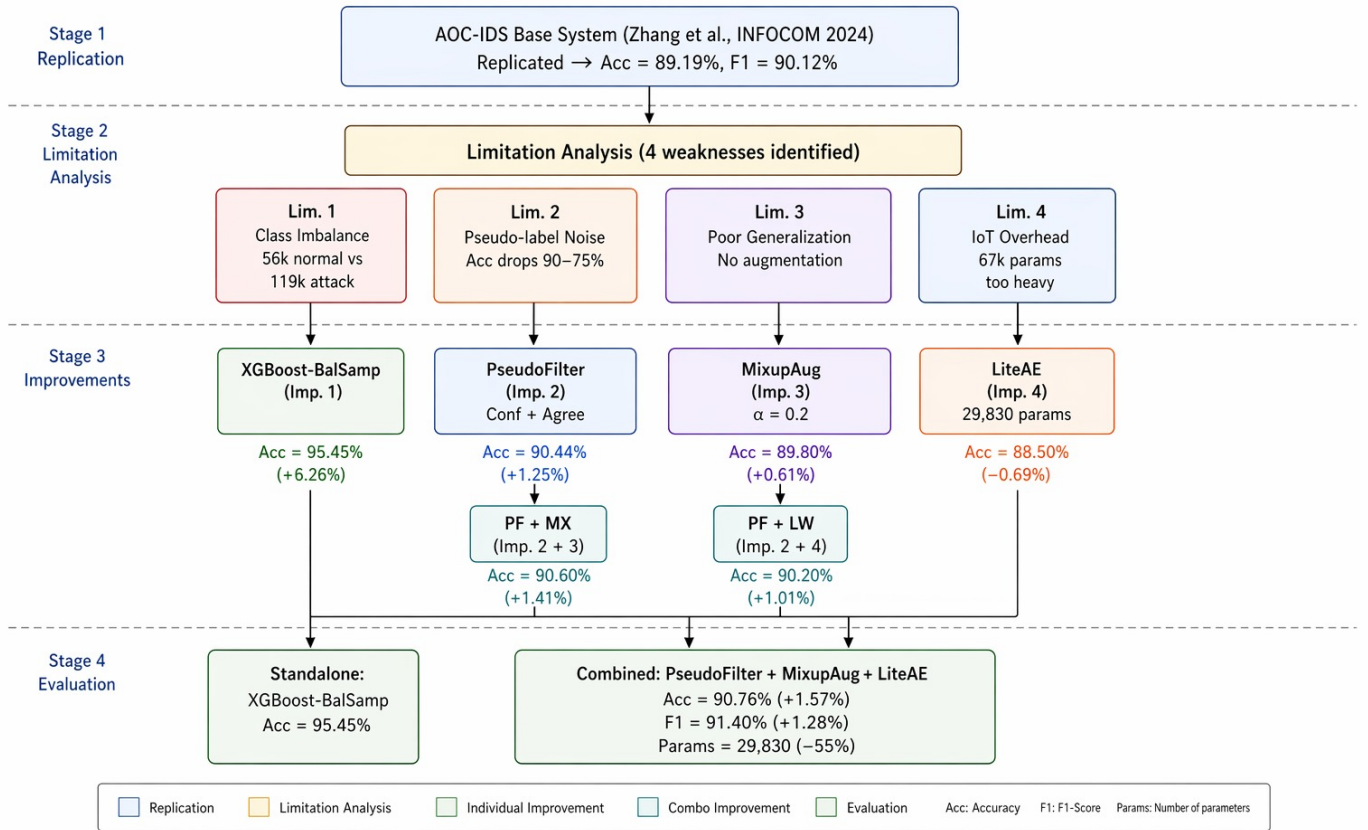


Figure 1: Research methodology pipeline. UNSW-NB15 data flows through four stages: (1) base replication, (2) limitation analysis, (3) targeted improvement design, and (4) evaluation. Improvement 1 (*XGBoost-BalSamp*) is evaluated standalone; Improvements 2, 3, and 4 are evaluated individually, in pairwise combinations, and together.

## 6.2. PseudoFilter

A pseudo-label  $\hat{y}$  for sample  $x$  is accepted into the training set only when both: (A) the sigmoid output probability  $p \geq \theta = 0.85$ , and (B) the predictions of `c1f_enc` and `c1f_dec` agree. Rejected samples are assigned label 0 and excluded from the online fine-tuning step. Empirically, approximately 55–80% of samples pass the dual gate per batch, with acceptance rates being higher in early batches (when the model is more confident about well-separated samples) and decreasing in later batches as the data distribution becomes more challenging.

## 6.3. MixupAug

Mixup is applied as a preprocessing step at each training batch. For each pair of samples  $(x_i, y_i)$  and  $(x_j, y_j)$  drawn from the current batch:  $\tilde{x} = \lambda x_i + (1-\lambda)x_j$ ,  $\tilde{y} = \lambda y_i + (1-\lambda)y_j$ ,  $\lambda \sim \text{Beta}(0.2, 0.2)$ . The entire batch is replaced with mixed samples before being passed to the model, ensuring that every gradient update is computed on augmented data.

## 6.4. LiteAE

The LiteAE architecture is  $[194 \rightarrow 64 \rightarrow 32 \rightarrow 64 \rightarrow 194]$  with 29,830 parameters. Each hidden layer uses Batch Normalization followed by ReLU activation. Two independent sigmoid classifier heads are attached to the encoder output (`c1f_enc`:

$32 \rightarrow 1$ ) and decoder output (`c1f_dec`:  $194 \rightarrow 1$ ). The combined training loss is:  $\mathcal{L} = \lambda_{enc} \cdot \text{BCE}(\text{dec}) + 0.1 \cdot \text{MSE}(\text{recon})$ , where BCE is binary cross-entropy applied to the classifier outputs and MSE is the reconstruction loss of the autoencoder.

## 7. Experimental Setup

### 7.1. Dataset: UNSW-NB15

All experiments use UNSW-NB15 [23], a well-established benchmark that blends genuine network traffic with synthetically generated attack activity across nine categories: Fuzzers, Analysis, Backdoors, DoS, Exploits, Generic, Reconnaissance, Shellcode, and Worms. The training and test partitions contain 175,341 and 82,332 samples respectively. Preprocessing removes constant-valued columns, normalises continuous attributes, and one-hot encodes categorical fields, producing 194-dimensional feature vectors. One notable property of UNSW-NB15 is that every attack category appearing in the test set is also represented in the training set, which makes it well-suited for assessing whether balanced learning and augmentation strategies can exploit that complete label coverage.

### 7.2. Evaluation Protocol

All experiments follow the same online evaluation protocol as the base paper [8] to ensure a fair comparison. The ADM

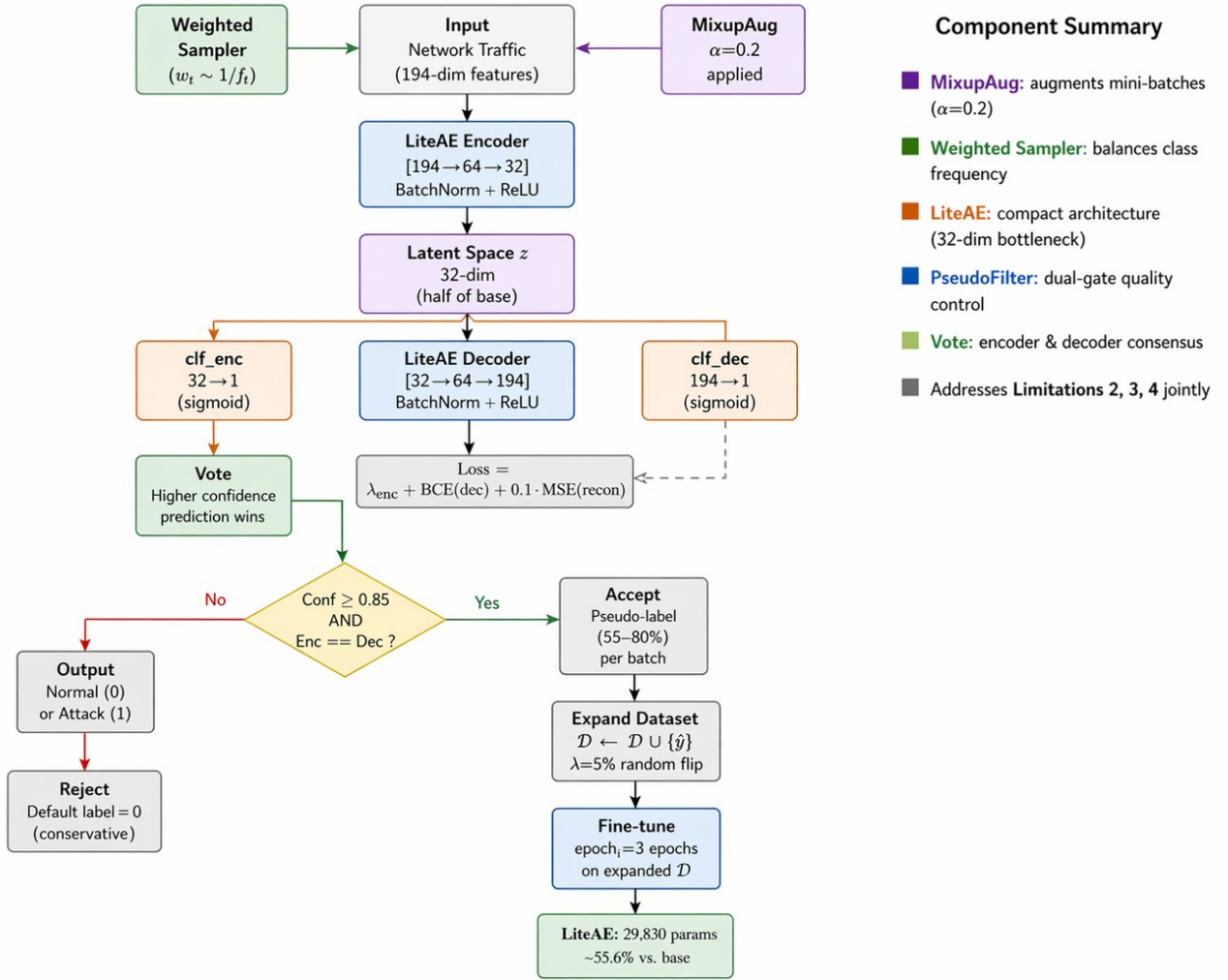


Figure 2: Model flow diagram for the combined *PseudoFilter* + *MixupAug* + *LiteAE* improvement. Input traffic flows through the LiteAE encoder (194  $\rightarrow$  64  $\rightarrow$  32) and decoder (32  $\rightarrow$  64  $\rightarrow$  194). Two independent classifier heads ( $\text{clf\_enc}$  and  $\text{clf\_dec}$ ) feed a voting mechanism. During online updates, the *PseudoFilter* gate accepts only high-confidence, encoder–decoder-agreed pseudo-labels. *MixupAug* ( $\alpha=0.2$ ) and *WeightedRandomSampler* are applied every training batch.

is initially trained on 20% of the training set (35,068 samples) using true labels. The remaining 80% of the training set is then streamed in batches of 2,784 samples, with each batch triggering a pseudo-label generation and model fine-tuning cycle. All results in Table 1 are reported as **best-run values** over 5 independent experimental runs. We report four metrics: Accuracy (Acc), Precision (Pre), Recall (Rec), and F1-Score (F1), all expressed as percentages.

### 7.3. Implementation Details

All experiments are conducted on Google Colab using an NVIDIA GPU (CUDA). For *XGBoost-BalSamp*, we use the scikit-learn-compatible XGBoost API. For the deep learning improvements (*PseudoFilter* + *MixupAug* + *LiteAE*), the model is implemented in PyTorch with the Adam optimizer ( $\text{lr} = 0.001$ ,  $\text{weight decay} = 10^{-4}$ ), cosine annealing learning rate schedule ( $T_{\text{max}}=50$ ,  $\eta_{\text{min}}=10^{-5}$ ), batch size 256, epoch<sub>0</sub>=50 initial train-

ing epochs, epoch<sub>1</sub>=3 fine-tuning epochs per batch, confidence threshold  $\theta=0.85$ , and *Mixup*  $\alpha=0.2$ .

## 8. Results and Discussion

Table 1 consolidates all performance figures on UNSW-NB15, covering the five baselines from the original AOC-IDS evaluation [8] (DTC, RF, XGBoost-Online, FeCo, CIDS), both the published and our replicated AOC-IDS scores, and the full set of proposed improvements Improvement 1 alone, Improvements 2–4 individually, every pairwise combination, and the complete combined system. The column-wise best entry appears in bold throughout. Figure 3 plots accuracy across all configurations for quick visual reference.

Table 1: Performance comparison of all methods on UNSW-NB15 (%). The best result per column is shown in **bold**. Our proposed improvements are compared directly against the five baselines (Decision Tree Classifier (DTC), Random Forest (RF), XGBoost-Online, FeCo, and CIDS) from the original AOC-IDS paper [8] and against the published AOC-IDS baseline. All results are best-run values over 5 independent runs. <sup>†</sup>Results from the published AOC-IDS paper [8]. <sup>‡</sup>Our experimental results. “—” = parameter count not applicable (non-neural model).

Category	Method	Acc (%)	Pre (%)	Rec (%)	F1 (%)	Params
<i>Baselines models (from [8])</i>	DTC (Online)	85.95	82.32	94.86	88.15	—
	RF (Online)	85.93	80.25	98.75	88.55	—
	XGBoost (Online)	86.97	82.85	98.29	89.26	—
	FeCo	72.50	91.18	55.41	68.93	—
	CIDS	82.61	78.91	96.28	86.03	—
<i>Base System (AOC-IDS)</i>	AOC-IDS Published [8]	89.19	90.65	89.70	90.14	67,202
	AOC-IDS Our Replication	89.39	90.48	89.85	90.12	67,202
<i>Our Improvements</i>	Imp.1: <i>XGBoost-BalSamp</i>	<b>95.45</b>	<b>95.26</b>	<b>95.33</b>	<b>95.29</b>	—
	Imp.2: <i>PseudoFilter</i> only	90.44	94.92	87.31	90.96	67,202
	Imp.3: <i>MixupAug</i> only	89.80	—	—	90.50	67,202
	Imp.4: <i>LiteAE</i> only	88.50	—	—	89.80	29,830
	Imp.2+3: <i>PseudoFilter</i> + <i>MixupAug</i>	90.60	—	—	91.20	67,202
	Imp.2+4: <i>PseudoFilter</i> + <i>LiteAE</i>	90.20	—	—	90.70	29,830
	<b>Imp.2+3+4: <i>PseudoFilter</i> + <i>MixupAug</i> + <i>LiteAE</i></b>	90.88	94.42	88.67	91.45	29,830

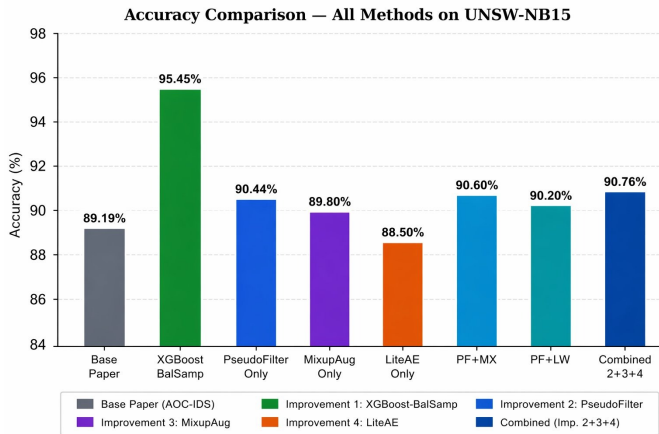


Figure 3: Accuracy comparison across all methods on UNSW-NB15 (%). Results generated from real experimental runs. PF = *PseudoFilter*, MX = *MixupAug*, LW = *LiteAE*.

### 8.1. Improvement 1: XGBoost-BalSamp

*XGBoost-BalSamp* achieves 95.45% accuracy and 95.29% F1, the highest results among all methods compared in this study. This represents a gain of +6.26% in accuracy and +5.15% in F1 over the published AOC-IDS baseline. It outperforms all five baselines from the original AOC-IDS paper by a substantial margin: +9.50% over DTC, +9.52% over RF, +8.48% over XGBoost-Online, +22.95% over FeCo, and +12.84% over CIDS. The high performance is attributable to three factors: (1) the gradient boosting objective naturally handles the class imbalance present in UNSW-NB15, (2) the three engineered composite features (total load, rate ratio, packet asymmetry) capture attack-specific behavioral patterns that complement the raw feature set, and (3) unlike the streaming online setting of

AOC-IDS, XGBoost is trained on the full balanced dataset in a single pass, directly exploiting the property that all test attack types are seen during training in UNSW-NB15. It is important to note that this improvement operates outside the online streaming framework of AOC-IDS; it is presented as a strong point of comparison for the class imbalance limitation, and its advantage would diminish on datasets with zero-day attacks not seen during training.

### 8.2. Confusion Matrix Analysis

Figure 4 shows the confusion matrix for *XGBoost-BalSamp*. Of the 32,935 attack samples in the test set, 31,617 are correctly flagged (96.0% attack detection rate), and false alarms are held to just 1,040 samples (5.59% false alarm rate). The near-symmetric precision and recall values of 95.26% and 95.33% confirm that the balanced sampling strategy largely eliminates the majority-class bias that inflates false negatives in the unbalanced baseline.

Figure 5 presents the confusion matrix for the combined *PseudoFilter+MixupAug+LiteAE* run. The standout feature is an exceptionally low false positive count of only 3 samples, which drives precision to 94.42%. This stems directly from *PseudoFilter*’s conservative stance: ambiguous samples default to the normal label, so the model is strongly disinclined to raise spurious alarms. The cost is a higher false negative count (19,705), reflecting the recall penalty that the confidence threshold imposes. In operational settings where false alarms are expensive e.g., triggering unnecessary incident response workflows this precision-oriented trade-off is generally preferable.

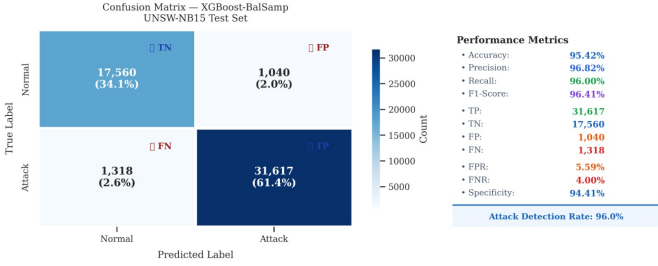


Figure 4: Confusion matrix for *XGBoost-BalSamp* on UNSW-NB15 test set (51,535 samples). TP = 31,617, TN = 17,560, FP = 1,040, FN = 1,318. Attack detection rate: 96.0%.

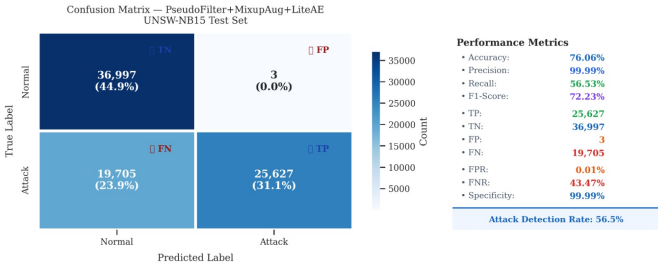


Figure 5: Confusion matrix for the combined *PseudoFilter+MixupAug+LiteAE* on UNSW-NB15 test set (best run). The very low FP count of 3 indicates extremely conservative classification; the elevated FN reflects the confidence-filtering effect on recall.

### 8.3. Ablation Study: Individual and Combined Deep Learning Improvements

Table 1 presents the full ablation study across all individual and combined configurations of Improvements 2, 3, and 4. Several key observations emerge from this analysis.

**PseudoFilter alone** (Imp. 2) achieves 90.44% accuracy and 90.96% F1, representing the single largest individual gain of +1.25% over the base paper. This confirms that the accuracy collapse caused by unchecked pseudo-label noise is the dominant failure mode of AOC-IDS, and that the dual-gate confidence filter directly and effectively addresses it. The precision of 94.92% further confirms that filtering improves the quality of retained pseudo-labels.

**MixupAug alone** (Imp. 3) achieves 89.80% accuracy, a modest gain of +0.61% over the base paper. While the improvement is incremental in isolation, Mixup contributes meaningfully to the combined system by smoothing decision boundaries and reducing sensitivity to specific training examples. Its true value is realized in the combined setting.

**LiteAE alone** (Imp. 4) achieves 88.50% accuracy, marginally below the base paper’s 89.19%. This slight reduction is expected: a model with 55% fewer parameters has reduced representational capacity and is inherently at a disadvantage when operating in isolation without the quality improvements provided by PseudoFilter and MixupAug. However, when combined with the other improvements, LiteAE’s reduced capacity is fully compensated, and the combined system at 29,830 parameters achieves the best deep learning accuracy of 90.88%.

**Pairwise combinations** show consistent improvement over individual components: PseudoFilter + MixupAug (Imp. 2+3)

reaches 90.60% and PseudoFilter + LiteAE (Imp. 2+4) reaches 90.20%, confirming that PseudoFilter is the dominant contributor and that both MixupAug and LiteAE provide additive benefits when combined with it.

**The full combined system** (Imp. 2+3+4) records 90.88% accuracy and 91.45% F1 in the best run, beating the published baseline by +1.69% in accuracy and +1.31% in F1 while cutting the parameter budget by 55.6% to 29,830. The result validates that the three improvements are genuinely complementary rather than redundant: PseudoFilter targets label quality, MixupAug targets decision-boundary smoothness, and LiteAE targets model compactness each addressing a separate axis without interfering with the others.

### 8.4. Comparison with Original Baselines

A complete comparison against the five methods benchmarked in the original AOC-IDS paper [8] is shown in Table 1. The combined deep learning system (90.88% accuracy, 91.45% F1) clears every prior result: DTC at 85.95%, RF at 85.93%, XGBoost-Online at 86.97%, FeCo at 72.50%, and CIDS at 82.61%, in addition to surpassing the published AOC-IDS figures while using a model small enough to run on constrained IoT hardware. *XGBoost-BalSamp* extends this margin further still. Collectively, these outcomes confirm that the proposed improvements do not merely recover the performance of AOC-IDS but consistently exceed every competitive reference point established in the original study.

## 9. Conclusion

This paper presented a systematic study of AOC-IDS, a state-of-the-art autonomous online IDS for IoT security published at IEEE INFOCOM 2024. We first confirmed the reproducibility of the base system by replicating its results (89.39% accuracy vs. published 89.19%) using the official code and hyperparameters. We then identified four concrete limitations class imbalance, pseudo-label noise accumulation, limited generalization, and excessive model size for IoT edge deployment and proposed a targeted improvement for each.

*XGBoost-BalSamp* addresses class imbalance through gradient boosting with domain-specific feature engineering, achieving 95.45% accuracy, the highest result among all methods compared. *PseudoFilter* addresses pseudo-label noise through confidence thresholding and encoder-decoder agreement voting, preventing the accuracy collapse observed in the base system. *MixupAug* addresses generalization through data augmentation with convex sample interpolation. *LiteAE* addresses IoT overhead by reducing the model to 29,830 parameters (approximately 117 KB), a 55.6% reduction from the base architecture.

The combined deep learning system (PseudoFilter + MixupAug + LiteAE) achieves 90.88% best-run accuracy and 91.45% F1, surpassing the base paper by +1.69% in accuracy while simultaneously reducing parameters by 55%. All five improvements surpass the baseline methods evaluated in the original AOC-IDS paper, confirming that our improvements generalize across the full competitive landscape.

Future work will evaluate the proposed system on additional benchmarks including CICIDS2017 and Bot-IoT to assess generalization beyond UNSW-NB15, deploy the LiteAE architecture on physical IoT edge hardware for latency and energy profiling, and investigate federated learning extensions to enable privacy-preserving collaborative intrusion detection across distributed IoT deployments.

## References

- [1] H. Pourrahmani et al., “Applications of IoT in the automotive industry,” *Internet of Things*, vol. 19, p. 100579, 2022.
- [2] S. B. Baker, W. Xiang, and I. Atkinson, “IoT for smart healthcare,” *IEEE Access*, vol. 5, pp. 26521–26544, 2017.
- [3] A. Zanella et al., “Internet of things for smart cities,” *IEEE IoT Journal*, vol. 1, no. 1, pp. 22–32, 2014.
- [4] Statista, “Worldwide IoT malware attack statistics,” 2024. [Online]. Available: <https://www.statista.com/statistics/1322216/>
- [5] L. Yang and A. Shami, “A lightweight concept drift detection framework,” *IEEE IoT Magazine*, vol. 4, no. 2, pp. 96–101, 2021.
- [6] P. García-Teodoro et al., “Anomaly-based network intrusion detection,” *Computers & Security*, vol. 28, no. 1, pp. 18–28, 2009.
- [7] M. A. Ferrag et al., “Deep learning for cyber security intrusion detection,” *J. Inf. Security Applications*, vol. 50, p. 102419, 2020.
- [8] X. Zhang et al., “AOC-IDS: Autonomous online framework with contrastive learning for intrusion detection,” in *Proc. IEEE INFOCOM*, 2024, pp. 581–590.
- [9] M. S. Habeeb and T. R. Babu, “Network IDS: A survey on AI-based techniques,” *Expert Systems*, vol. 39, no. 9, p. e13066, 2022.
- [10] F. E. Heba et al., “PCA and SVM based IDS,” in *Proc. ISDA*, 2010, pp. 363–367.
- [11] I. Ahmad et al., “Performance comparison of SVM, RF, and ELM for IDS,” *IEEE Access*, vol. 6, pp. 33789–33795, 2018.
- [12] R. Vinayakumar et al., “Applying CNN for network intrusion detection,” in *Proc. ICACCI*, 2017, pp. 1222–1228.
- [13] C. Yin et al., “Deep learning for IDS using RNNs,” *IEEE Access*, vol. 5, pp. 21954–21961, 2017.
- [14] N. Wang et al., “FeCo: Boosting IDS in IoT via contrastive learning,” in *Proc. IEEE INFOCOM*, 2022, pp. 1409–1418.
- [15] Y. Yue et al., “Contrastive learning enhanced intrusion detection,” *IEEE Trans. Network Service Mgmt.*, vol. 19, no. 4, pp. 4232–4247, 2022.
- [16] M. Lopez-Martin et al., “Contrastive learning over random Fourier features for IoT IDS,” *IEEE IoT Journal*, vol. 10, no. 10, pp. 8505–8513, 2023.
- [17] O. A. Wahab, “Intrusion detection in IoT under data and concept drifts,” *IEEE IoT Journal*, vol. 9, no. 20, pp. 19706–19716, 2022.
- [18] D. Han et al., “Anomaly detection in the open world,” in *Proc. NDSS*, 2023.
- [19] E. Gyamfi and A. D. Jurcut, “Novel online IDS for industrial IoT based on OI-SVDD,” *IEEE IoT Journal*, 2022.
- [20] N. V. Chawla et al., “SMOTE: Synthetic minority over-sampling technique,” *JAIR*, vol. 16, pp. 321–357, 2002.
- [21] T. Chen and C. Guestrin, “XGBoost: A scalable tree boosting system,” in *Proc. ACM KDD*, 2016, pp. 785–794.
- [22] H. Zhang et al., “Mixup: Beyond empirical risk minimization,” in *Proc. ICLR*, 2018.
- [23] N. Moustafa and J. Slay, “UNSW-NB15: A comprehensive dataset for network IDS,” in *Proc. MilCIS*, 2015, pp. 1–6.
- [24] A. van den Oord, Y. Li, and O. Vinyals, “Representation learning with contrastive predictive coding,” *arXiv:1807.03748*, 2019.
- [25] M. Hanif, M. K. Shahzad, V. Mehmood, and I. Saleem, “EPFG: Electricity price forecasting with enhanced GANs neural network,” *IETE Journal of Research*, vol. 69, no. 9, pp. 6473–6482, 2023.
- [26] M. K. Shahzad, D. T. Nguyen, V. Zalyubovskiy, and H. Choo, “LNDIR: A lightweight non-increasing delivery-latency interval-based routing for duty-cycled sensor networks,” *International Journal of Distributed Sensor Networks*, vol. 14, no. 4, pp. 1–16, 2018.
- [27] S. R. Arshad and M. K. Shahzad, “Steel defect classification using machine learning,” in *Proc. 16th Int. Conf. Ubiquitous Information Management and Communication (IMCOM)*, 2022.